JOURNAL OF MATERIALS SCIENCE 23 (1988) 2387–2393

Thermodynamic properties of iron doped beta″-alumina by e.m.f. measurements with beta-alumina electrolytes

T. Y. TSENG
Institute of Electronics, National Chiao-Tung University, Hsinchu, Taiwan
R. W. VEST
Purdue University, West Lafayette, Indiana 47907, USA

Thermodynamic studies of the non-stoichiometric iron doped beta″-alumina (IDβ'') phase were carried out by electrochemical measurements coupled with coulometric titration using the cell Na_{liq}/Li β''-alumina/IDβ''. Hot pressing and glass sealing techniques were developed and employed to obtain a suitable and stable Li β''-alumina/IDβ'' interface. The equilibrium e.m.f. of the cell was determined as a function of sodium concentration over the temperature range 444 to 523 K. The range of sodium concentrations over which the IDβ'' phase is stable was also determined. The relative partial molar thermodynamic quantities of sodium, $\overline{\Delta G}_{Na}$, $\overline{\Delta H}_{Na}$, and $\overline{\Delta S}_{Na}$ in IDβ'' alumina as a function of sodium concentration were obtained from cell e.m.f. data.

1. Introduction

It has been established that the iron doped beta″-alumina (IDβ'') has a large range of homogeneity for sodium, and it has been suggested that IDβ'' may be a good candidate for solid solution electrodes for electrochemical devices utilizing sodium β-alumina type electrolyte [1]. The potential applications to electrochemical devices make a fundamental understanding of the thermodynamic properties of this solid solution electrode highly desirable.

The application of a β-aluminas solid electrolytes galvanic cell coupled with coulometric titrations of thermodynamic measurements has been studied in a number of two-component [2, 4] and three-component systems [5, 6]. Dudley, Steele and Howe [6] attempted to study the thermodynamic properties of the non-stoichiometric potassium ferrite phase with the β-alumina structure using the coulometric titration technique. They obtained the completely reversible cell e.m.f. as a function of potassium content at 523 K from a cell of the type

$$K_{liq}/K\ \beta\text{-alumina}/K\text{-ferrite}$$

which was sealed in a Pyrex enclosure filled with pure and dried argon to prevent changes in the oxygen content of K-ferrite during the titration. Unfortunately, they had difficulty in maintaining a good ionic contact between the potassium half-cell and the ferrite using a tungsten spring loaded electrode. A trace of $KAlCl_4$–$AlCl_3$ eutectic was employed to improve this contact. They claimed that the thermodynamic properties, enthalpy and entropy, will be reported elsewhere. The thermodynamic properties of sodium-intercalated tantalum disulphide (Na_xTaS_2) and sodium-intercalated titanium disulphide (Na_xTiS_2) have been investigated electrochemically using propylene carbonate-based electrolyte for measurements at 300 K and β- or β''-alumina electrolyte for measurements at 435 and 495 K [5]. Nagelberg and Worrell reported the sodium chemical potential and standard free energy of intercalation for Na_xTaS_2 and Na_xTiS_2 as functions of composition x at 300 K. However, they could not obtain the partial molar enthalpy and partial molar entropy from their data of temperature dependence of open circuit voltage. It was felt that a revision of their solid electrolyte cell design was probably necessary.

In the present study, hot pressing and glass sealing techniques were developed and employed to obtain a suitable and stable Li β''-alumina/IDβ'' interface. Thermodynamic properties of IDβ'' were determined by electrochemical cell measurements coupled with coulometric titrations.

2. Experimental procedure

2.1. Material preparation

The thin wall closed-end sodium β''-alumina electrolyte tubes having the dimensions of 9.4 mm o.d., 0.7 mm wall diameter and 152 mm length were supplied by General Motors Research Laboratories, Warren, Michigan. The β''-alumina tubes were fabricated from spray-dried powders of composition 0.8% Li_2O–9.0% Na_2O–90.2% Al_2O_3 by weight [7]. The X-ray analysis showed the electrolyte tube to consist of β'' phase with a trace of β phase.

IDβ'' cathode electrode samples were prepared within the single phase field established by the earlier work [1]. Compositions of IDβ'' cathode material were

0022–2461/88 $03.00 + .12

TABLE I Annealing conditions of IDβ'' specimens

Cell	Fabrication method	IDβ'' weight (g)	Annealing condition			$Fe^{+2}/Fe^{+2} + Fe^{+3}$	X-ray results
			Temp (°C)	Atmosphere	Time (h)		
A	hot press	IDβ''(1) = 0.3286	600	air	96	2.1×10^{-2}	IDβ'' phase plus some of Fe_2O_3 phase
B	glass sealing	IDβ''(2) = 0.3900	610	9.6 p.p.m. CO in CO_2	90	8.1×10^{-2}	IDβ'' single phase

fabricated according to the formula

$$Na_2O \cdot Y(Al_{1-x}Fe_x)_2O_{3-m} \quad (1)$$

where

$$x = \frac{\text{moles iron}}{\text{moles iron + moles aluminum}}$$

$$Y = \frac{\text{moles iron + moles aluminum}}{\text{moles sodium}}$$

and m is a parameter that varies with the valence state of the iron. The dependence of the ratio of moles ferrous iron to moles iron, $(Fe^{+2}/Fe^{+2} + Fe^{+3})$, in non-stoichiometric IDβ'' phase on the oxygen partial pressure and temperature has been determined [8]. It was found that electronic conductivity was greatest in the non-stoichiometric potassium ferrite phase with the largest Fe^{+2} content [9]. Therefore, if the IDβ'' samples are annealed at a certain oxygen partial pressure and temperature which will increase Fe^{+2} content, less equilibration time will be required to achieve equilibrium cell e.m.f. in the coulometric titration studies. Accordingly, two cells in this study after fabrication were annealed at the known temperature and oxygen partial pressure listed in Table I. A gas mixture of CO_2–CO was placed on the same level with the IDβ'' electrode. After a reasonable period of time, the specimens were quenched by pulling them out of the furnace. The ratio, $Fe^{+2}/Fe^{+2} + Fe^{+3}$, in the ID$\beta''$ pellets was determined using the chemical analysis technique developed by Pastor [8] to obtain the $Fe^{+2}/Fe^{+2} + Fe^{+3}$ data in the IDβ'' electrode on the bottom of the tube. Table I lists the annealing conditions and $Fe^{+2}/Fe^{+2} + Fe^{+3}$ ratio for different specimens. The value of m in Equation 1 could be calculated from the $Fe^{+2}/Fe^{+2} + Fe^{+3}$ ratio obtained by chemical analysis. However, in order to depict the β'' structure, a chemical formula, which describes one sodium layer and one spinel block in a unit cell, given in the earlier work [1], was used

$$Na_zO \cdot 4\{Al_{1-x}(Fe_\phi^{+2}Fe_{1-\phi}^{+3})_x\}_{3-\sigma}V_\sigma O_4 \quad (2)$$

where

x = moles iron/(moles iron + moles aluminum)
ϕ = moles of ferrous iron/moles iron $(Fe^{+2} + Fe^{+3})$
z = number of sodium ion per conducting layer
V = vacancy on the aluminum sublattice
σ = number of vacancies

Table II lists the two different chemical formulae for cell specimens.

The anode material used in this work was pure sodium obtained from a commercial source (Mallinckrodt Chemical Works, St Louis, MO.). The purification of as-received solid sodium was carried out in a hot trapping device inside a dry box to remove impurities, such as sodium oxide and sodium hydroxide formed by reactions with trace amounts of oxygen and water vapour in the dry box atmosphere. Stainless steel wire which does not react with liquid sodium at low oxygen partial pressure was used as the electronic conductor at the liquid sodium anode.

2.2. Cell construction

A cell holder was designed and constructed based on the Li β''-alumina closed end tube, as shown in Fig. 1. In order to maintain the open end of the tube below 100° C, cooling water was circulated through the $\frac{1}{4}''$ o.d. copper tubing wound along the outside of a brass tube. Moreover, the cell holder was fitted in the water cooled furnace inside the dry box. The temperature of the IDβ'' specimen was maintained constant by placing a control thermocouple near the heating element of the furnace, and by shielding the specimens with alumina radiation shields. The temperature of the furnace was controlled with a digital setpoint controller (Barbor-Colman Comp., Ill., USA) and could be kept constant to within 1° C over long periods.

Hot pressing and glass sealing techniques were developed and employed to obtain the suitable interfacial contacts between the IDβ'' and Li β''-alumina tube. In the hot pressing process, the optimum

TABLE II Chemical formulae of IDβ'' specimens

Specimens	Chemical formula (1)	Chemical formula (2)
IDβ''	$Na_2O \cdot 5.5[(Al_{0.65}Fe_{0.35})_2O_{2.9927}]$	$Na_{1.95+k}O \cdot 4[Al_{0.65}(Fe^{+2}_{0.021 + 0.2667k} Fe^{+3}_{0.979 - 0.2667k})_{0.35}]_{2.678}V_{0.322}O_4$
IDβ''(2)	$Na_2O \cdot 5.5[(Al_{0.55}Fe_{0.45})_2O_{2.9636}]$	$Na_{1.96538+k}O \cdot 4[Al_{0.55}(Fe^{+2}_{0.081035 + 0.20558k} Fe^{+3}_{0.918965 - 0.20558k})_{0.45}]_{2.7024}V_{0.2976}O_4$

Note: k is a compositional factor corresponding to the amount of sodium ions added into or removed from the IDβ'' cathodes.

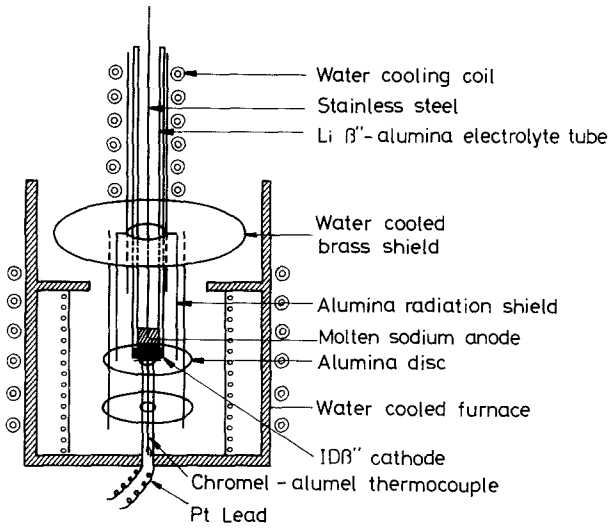

Figure 1 Experimental set-up of cell.

parameters of time, temperature and applied pressure were selected by trial and error. The optimum process for obtaining a suitable interface between electrode and electrolyte is given in [10]. In the glass sealing process, a sealing glass used for obtaining a connection between Li β''-alumina and IDβ'' was developed according to the following requirements: (1) the sealing glass should contain a large amount of sodium to be a good sodium ionic conductor, but should provide no driving force for sodium diffusion between the sealing glass and IDβ'' pellet. (2) the thermal expansion coefficient of the sealing glass should match those of Li β''-alumina and IDβ'' alumina. (3) it should have a suitable melting point for fabrication. A glass composition of 15 w/o Na_2O, 40 w/o SiO_2 and 45 w/o B_2O_3 was appropriate as such a sealing glass for Li β''-alumina to IDβ'' ($Na_2O \cdot 5.5(Al_{0.55}Fe_{0.45})_2O_3$) connection [10]. The sealing glass film between the Li β''-alumina and IDβ'' will not influence the final thermodynamic data if the thickness of the sealing glass is very small with respect to the thickness of the Li β''-alumina as described in [10].

The thermodynamic studies of IDβ'' were carried out in controlled inert gas atmospheres. In order to ensure that this four-component system being studied was thermodynamically well defined and to prevent the liquid sodium anode from reacting explosively in moist air, a dry box (Kewaunee Scientific Equipment, MI, USA.) was installed and modified for this investigation. The dry box was designed to provide maximum purity of the inert gas atmosphere of nitrogen, argon or helium and could reduce the contamination levels of moisture and oxygen within the enclosure to less than 1 p.p.m. Therefore, the $Fe^{+2}/Fe^{+2} + Fe^{+3}$ ratio will not change due to oxidation in the dry box at low temperature. Ultra high purity helium gas (99.999%) was used as the cover gas inside the dry box. A sodium–potassium liquid metal was used as an oxygen getter to reduce the O_2 content of the helium to the level required in the experiment.

2.3. Electrical measurements

The cells with IDβ'' cathodes of different compositions are

$$Na_{liq}/Li\ \beta''\text{-alumina/ID}\beta''(1) \quad (A)$$

$$Na_{liq}/Li\ \beta''\text{-alumina/ID}\beta''(2) \quad (B)$$

The compositions of IDβ''(1) and IDβ''(2) listed in Table II were used to determine the thermodynamic properties of IDβ'' cathodes as a function of sodium content in the cathodes and temperature by coulometric titration. Coulometric titrations were carried out at temperatures between 444 and 523 K by passing constant currents for measured times between the sodium anode and the IDβ'' cathode. Considering the rate and extent of polarization during the titration and a reasonable rate for polarization decay after titration, different titration currents from 10 $\mu A\,cm^{-2}$ to 42 $\mu A\,cm^{-2}$ were used in the two cells with different Fe^{+2} content cathodes. In the discharge direction, the sodium ions were added into the IDβ'' cathodes and charge compensation was maintained by the conversion of an appropriate number of trivalent iron atoms to divalent iron atoms. Due to the high ionic and electronic conduction of IDβ'', sodium ions are expected to distribute rapidly throughout the whole volume of IDβ'' cathode. The electrode reaction at the sodium anode is

$$Na \rightarrow Na^+ + e^-$$

and that at the IDβ'' cathode is

$$Fe^{+3} + e^- + Na^+ \rightarrow Fe^{+2} + Na^+$$

so that the overall cell reaction is

$$Na + Fe^{+3} \rightarrow Na^+ + Fe^{+2}$$

The reverse reactions occur for sodium transport in the opposite direction. After passing a known number of Coulombs, the sodium content of IDβ'' was determined by the application of Faraday's law. Each cell was allowed to equilibrate until the cell e.m.f. was constant with time after turning off the current. After reaching a steady value, the cell e.m.f. would remain constant within 1 mV for several days. The equilibration times were found to be vastly different from cell to cell. The IDβ'' with 2.1% Fe^{+2} used in cell (A) exhibited significant polarization at 523 K with current densities as low as 10.4 $\mu A\,cm^{-2}$. It took about eight days to reach a steady value. However, the IDβ'' with 8.1% Fe^{+2} used in cell (B) exhibited insignificant polarization with a current density 42 $\mu A\,cm^{-2}$ at 523 K after continuous sodium removal for several days. The results are consistent with the view that the electronic conductivity of iron-containing spinel is proportional to the Fe^{+2} content in the sample and the conductivity is probably due to a small polaron mechanism involving electron hopping between Fe^{+2} and Fe^{+3} in octahedral sites [6, 11–13].

After recording the e.m.f. value, the temperature was slowly lowered to the next temperature of interest. At each temperature, the cell was allowed to equilibrate, the polarity of the electrodes was reversed, and the cell e.m.f. was corrected for the thermoelectric effect between the platinum and stainless steel.

3. Results and discussion

3.1. E.m.f. of coulometric titration cells

The measured e.m.f.s for cell (A) with IDβ''(1)

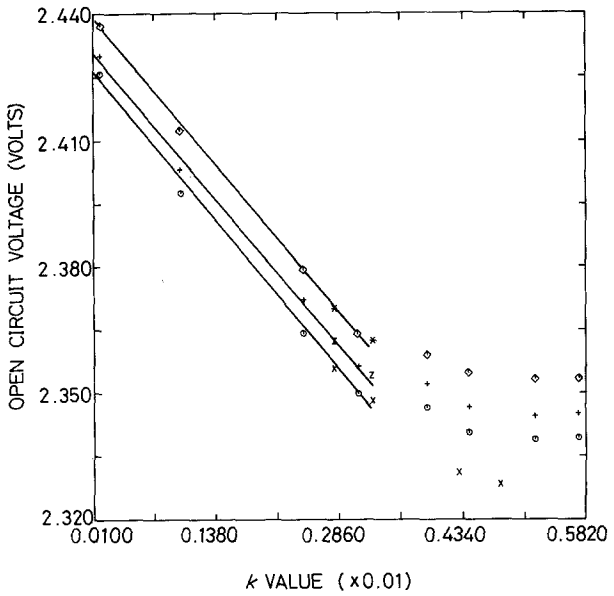

Figure 2 Compositional variation of e.m.f. with k in IDβ''(1) using cell (A) at three different temperatures. 523 K: ⊙ discharge, x charge, 487 K: + discharge, Z charge, 444 K: ◇ discharge, * charge.

electrodes of variable compositions at 523 K, 487 K and 444 K are shown in Fig. 2. Over the temperature range investigated, all the titration curves exhibited a similar composition dependence. As can be seen, the open circuit voltage decreased from 2.4258 V ($k = 0$) to 2.3480 ($k = 0.003\,274$) at 523 K, from 2.4303V ($k = 0$) to 2.3540 ($k = 0.003\,274$) at 487 K and from 2.437 2V ($k = 0$) to 2.3625V ($k = 0.003\,274$) at 444 K. Over this range, the open circuit voltage exhibited linear variation with the compositional parameter k in the chemical formula (2) of IDβ''(1) listed in Table II. The straight lines shown in Fig. 2 were obtained by a least-squares analysis, and are represented by Equations 3, 4 and 5.

At 523 K

$$E(\mathrm{V}) = (2.4187 \pm 0.0015) - (22.0545 \pm 0.6031)k \quad (3)$$

At 487 K

$$E(\mathrm{V}) = (2.4246 \pm 0.0015) - (21.8387 \pm 0.5475)k \quad (4)$$

At 444 K

$$E(\mathrm{V}) = (2.4337 \pm 0.0017) - (22.2367 \pm 0.6519)k \quad (5)$$

The voltage plateaus observed at $k > 0.0036$ in Fig. 2, are probably indicative of a phase transition or a third phase beyond β''-alumina and Fe_2O_3 phases. In the charge direction it was found the voltage was not reversible in the plateau regions, but it was reversible in the linear region as shown in Fig. 2. This hysteresis could probably be due to the strain energy and internal surface energy set up by the additional phase or phases. Kennedy and Samuels [14] investigated galvanic cells of the form

$$\mathrm{Na}/\beta\text{-alumina}/\mathrm{Na_2O} \cdot 11(\mathrm{Fe}_x\mathrm{Al}_{2-x}\mathrm{O}_3)$$

where x varied between 0.9 and 1.2 at 120° C. The

TABLE III E.m.f. of cell (A) as a function of temperature

k value	e.m.f. value, E (V)
0	$(2.5013 \pm 0.0049) - (1.448 \pm 0.101) \times 10^{-4} T$ (K)
0.000 973	$(2.4950 \pm 0.0078) - (1.869 \pm 0.160) \times 10^{-4} T$ (K)
0.002 443	$(2.4641 \pm 0.0072) - (1.904 \pm 0.149) \times 10^{-4} T$ (K)
0.002 810	$(2.4499 \pm 0.0012) - (1.799 \pm 0.025) \times 10^{-4} T$ (K)
0.003 106	$(2.4438 \pm 0.0012) - (1.799 \pm 0.025) \times 10^{-4} T$ (K)
0.003 274	$(2.4440 \pm 0.0043) - (1.840 \pm 0.089) \times 10^{-4} T$ (K)

cathode material $Na_2O \cdot 11(Fe_xAl_{2-x}O_3)$ was detected as β-alumina with some Fe_2O_3 in their X-ray patterns. The cell reaction in their galvanic cell is supposed to be the same as in our study. They reported that the initial open-circuit voltages varied between 2.37 and 2.45 V values comparable to the results shown in Fig. 2. The e.m.f. of cell (A) was determined as a function of temperature and the results from the linear region in Fig. 2 were employed to obtain the relationship between E and T through a linear regression analysis of the data as listed in Table III.

Fig. 3 shows the equilibrium cell e.m.f. at 523 K, 487 K and 444 K, as a function of sodium content calculated from the charge passed during each titration and the mass of the specimen using the formula (2) of IDβ''(2) listed in Table II together with chemical analysis of sample at the starting composition. As can be seen, excellent reproducible data were obtained over four discharge and three charge cycles. The e.m.f. varies almost linearly with sodium content over the compositional range from $k = -0.2685$ to $k = 0.30$. This material has good charge storage capacity because of the wide homogeneous composition range for the incorporation of sodium. Whittingham has suggested that the topochemical reaction plays an important role in the electrochemical reaction [15]. Based on this suggestion, the good reversibility of the cell based on

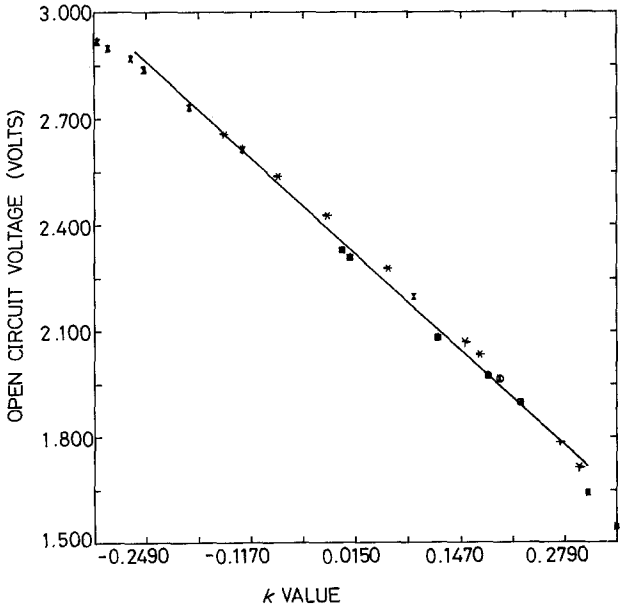

Figure 3 Compositional variation of e.m.f. with k in IDβ''(2) using cell (B) at three different temperatures. 523 K: □ first discharge, ◇ second discharge, ⋉ third discharge, * fourth discharge, O first charge, | second charge, ⋈ third charge, 487 K: △ first discharge, Y second discharge, ⊕ third discharge, O fourth discharge, × first charge, * second charge, | third charge, 444 K: + first discharge, − second discharge, | third discharge, ⧺ fourth discharge, Z first charge, − second charge, ∧ third charge.

sodium metal could be explained by the β''-alumina crystal structure, which remains essentially unchanged during the reaction; no chemical bonds are broken in the host β''-alumina matrix during insertion or removal of sodium.

Fig. 3 shows the small temperature dependence of cell e.m.f. over the temperature range 523–444 K and the ranges of linear dependence of cell e.m.f. on k values are the same for the three different temperatures. Comparing Figs 2 and 3, it is seen that the Fe^{+2} content greatly influences the stoichiometric range of IDβ'' alumina. Higher electronic conductivity due to the increasing pairing probability of Fe^{+2} and Fe^{+3} in octahedral sites is probably responsible for this different stoichiometric range of IDβ'' alumina; on the other hand, the defects associated with the changing Fe^{+2} content might also contribute to the wider stoichiometric range. From the point of view of engineering application, it will help in determining the allowable operational range of the electrochemical device with an IDβ'' alumina electrode of given composition.

3.2. Thermodynamic treatment of the data

The useful thermodynamic quantities of IDβ'' alumina can be obtained from the experimental data presented in Figs 2 and 3. The activity of sodium in IDβ'' alumina, a_{Na}, can be evaluated from these data and the equation

$$E = \frac{-RT}{F} \ln a_{Na} \tag{6}$$

The plots of $-\log a_{Na}$ against k at 444 K, 487 K, and 523 K can be obtained for IDβ''(1) sample in cell (A) and for IDβ''(2) sample in cell (B); they show a linear relationship with the stoichiometric parameter k over the temperature range of interest [10]. The process of sodium removal from or addition to the non-stoichiometric IDβ' alumina can be considered as a solution process. The partial molar free energy of solution of sodium in IDβ'' alumina, $\overline{\Delta G}_{Na}$ can be

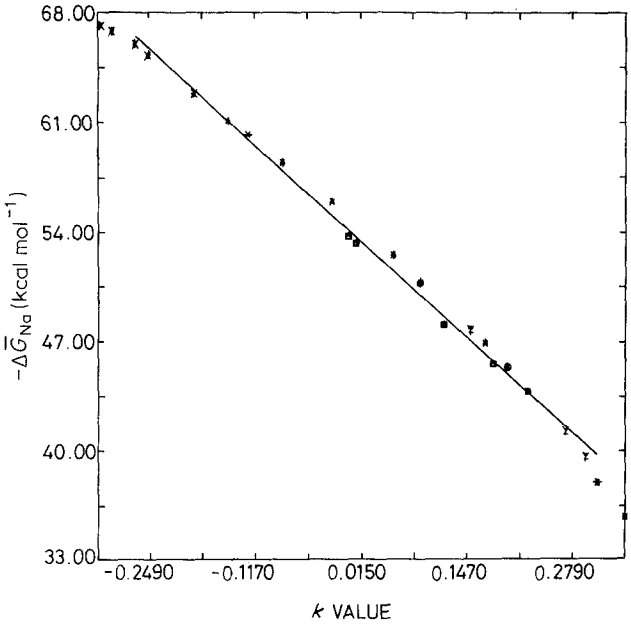

Figure 5 Relative partial molar free energy of sodium in IDβ''(2) as a function of composition at three different temperatures. 523 K: □ first discharge, ◇ second discharge, ⋉ third discharge, * fourth discharge, ○ first charge, ↑ second charge, ⋈ third charge. 487 K: △ first discharge, Y second discharge, ⊕ third discharge, ○ fourth discharge, × first charge, * second charge, ↑ third charge. 444 K: + first discharge, Z second discharge, → third discharge, ← fourth discharge, ↓ first charge, ∧ second charge, ⧗ third charge.

determined from the above mentioned log a_{Na} against k isotherms and the equation

$$\overline{\Delta G}_{Na} = RT \ln a_{Na} \tag{7}$$

$\overline{\Delta G}_{Na}$ varies as a function of composition, as shown in Fig. 4 for IDβ''(1) cell (A), and in Fig. 5 for IDβ''(2) in cell (B). The partial molar free energy of sodium in solution, $\overline{\Delta G}_{Na}$, is a convenient parameter to compare the energy storage capabilites of the IDβ'' alumina as a battery cathode. The larger the partial molar free energy of sodium in solution, the larger will be the energy storage capacity per mole of the electrode.

The partial molar enthalpy of solution of sodium in

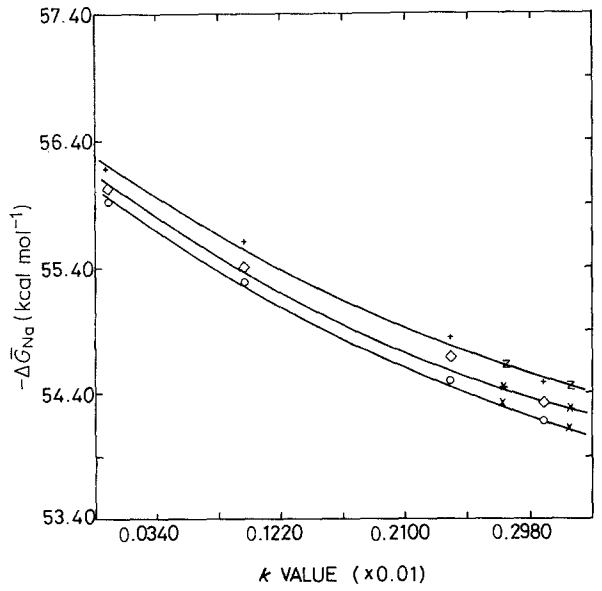

Figure 4 Relative partial molar free energy of sodium in IDβ''(1) as a function of composition at three different temperatures. 523 K: ○ discharge, × charge, 487 K: ◇ discharge, * charge. 444 K: + discharge, Z charge.

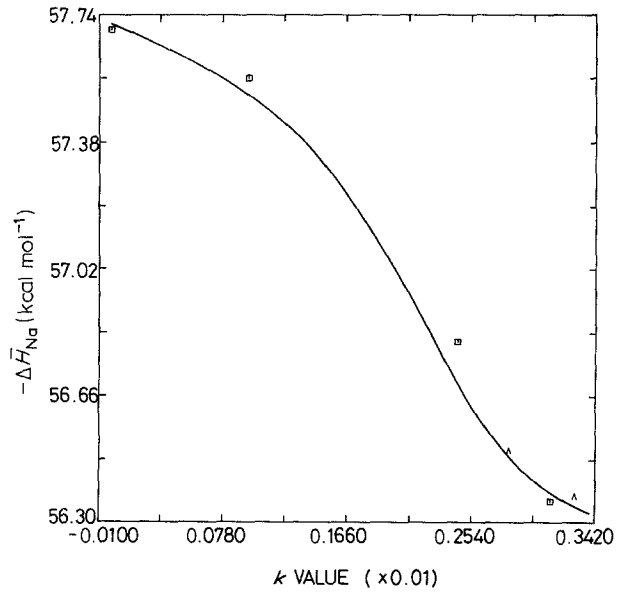

Figure 6 Relative partial molar enthalpy of sodium in IDβ''(1) as a function of composition at temperature range of 444–523 K. □ discharge, ∧ charge.

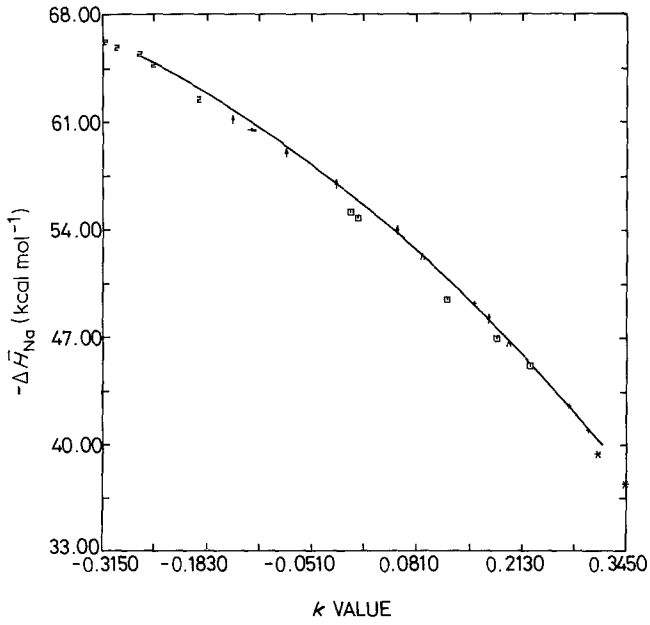

Figure 7 Relative partial molar enthalpy of sodium in IDβ''(2) as a function of composition at the temperature range of 444–523 K. □ first discharge, + second discharge, → third discharge, * fourth discharge, ∧ first charge, ↑ second charge, ƨthird charge.

IDβ'' alumina may be obtained as a function of composition, provided the IDβ'' solution is homogeneous over the whole temperature range, from the slope of log a_{Na} against $1/T$ plots since

$$\overline{\Delta H}_{Na} = \frac{\partial(\overline{\Delta G}_{Na}/T)}{\partial(1/T)} = \frac{\partial(\ln a_{Na})}{\partial(1/T)} R \qquad (8)$$

A linear regression analysis of previously given values of log a_{Na} against $1/T$ data at constant values of k within the IDβ'' phase region was carried out using a computer. In order to obtain $\overline{\Delta H}_{Na}$ for a given value of k, the calculated slope was multiplied by 4.576. The $\overline{\Delta H}_{Na}$ values obtained in this manner are shown in Fig. 6 for IDβ''(1) in cell (A), and in Fig. 7 for IDβ''(2) in cell (B). The relative partial molar heat of addition of sodium increases in a non-linear manner with the composition parameter k within the homogeneous IDβ'' alumina phase for the IDβ'' alumina in cell (A) and cell (B). Endo *et al.* [16] interpreted the thermodynamic data of $Pr_{1-y}Gd_yO_{1.5+x}$ by assuming that the excess oxygen atoms randomly occupy the Z site of the C-type (bixbyite) structure without any ordering. According to their discussion, the enthalpy change $H(x)$ is expressed by

$$H(x) = -2N(\varepsilon x + n\omega x^2) \qquad (9)$$

where N is Avogadro's number, ε the energy required for introducing an oxygen atom into the Z site to form an O_Z^{2-} ion and two Pr^{4+} ions converted from Pr^{3+} ions; n the number of neighbouring sites of an O_Z^{2-} ion and ω the interaction energy of two adjacent O_Z^{2-} ions.

When ε and ω are constant the plot of partial molar enthalpy dH/dx against x is a straight line as can be seen from Equation (9). Endo *et al.* obtained a parabolic curve for dH/dx against x, by assuming that ε and ω change with the volume of the crystal. In the present case, one may propose a similar model to explain the non-linear behaviour shown in Figs 6 and 7. However, the present level of understanding of the

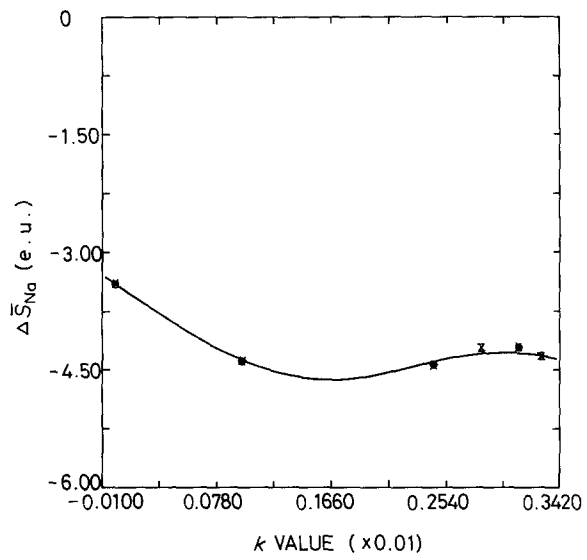

Figure 8 Relative partial molar entropy of sodium in IDβ''(1) as a function of composition at three different temperatures 444 K: ○ discharge, + charge, 487 K: * discharge, Z charge, 523 K: ○ discharge, × charge.

defect structure in IDβ'' alumina is not sufficient to attempt this type of analysis for sodium ions in IDβ'' alumina.

From $\overline{\Delta G}_{Na}$ and $\overline{\Delta H}_{Na}$, the partial molar entropy, $\overline{\Delta S}_{Na}$, may be calculated, using the relationship

$$\overline{\Delta S}_{Na} = \frac{\overline{\Delta H}_{Na} - \overline{\Delta G}_{Na}}{T} \qquad (10)$$

$\overline{\Delta S}_{Na}$ varies as a function of composition as shown in Fig. 8 for IDβ''(1) in cell (A) and in Fig. 9 for IDβ''(2) in cell (B). As can be seen, all $\overline{\Delta S}_{Na}$ values in the homogeneous range of IDβ'' alumina show non-linear behaviour, which is probably due to the non-random distribution of sodium ions on the available sites in the IDβ'' alumina structure $\overline{\Delta S}_{Na}$ varies almost

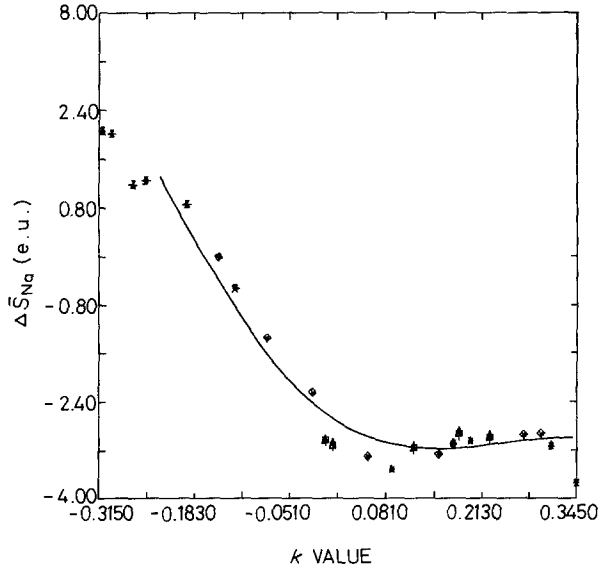

Figure 9 Relative partial molar entropy of sodium in IDβ''(2) as a function of composition at three different temperatures. 523 K: ↓ first discharge, ◇ second discharge, ⋉ third discharge, ↑ fourth discharge, ○ first charge, * second charge, ⋈ third charge, 487 K: △ first discharge, Y second discharge, ⊕ third discharge, ○ fourth discharge, × first charge, Z second charge, ← third charge. 444 K: □ first discharge, + second discharge, → third discharge, * fourth discharge, ∧ first charge, ↑ second charge, ƨ third charge.

linearly with the stoichiometric parameter k in the region $k < 0.15$ as shown in Fig. 9. The lowering of the entropy term at higher k value might be interpreted to mean a continuous increase of order on the sodium sublattice. The entropy values at $k > 0.15$ shown in Fig. 9 were found to be nearly independent of sodium concentration. The configurational entropy should be an appreciable fraction of the total $\overline{\Delta S}_{Na}$ in IDβ'' alumina, and might be evaluated on the basis of the site occupations and nearest-neighbour pair interactions. The number of Na^+–Na^+ pairs increases with increasing k value; therefore, there would be higher pair repulsion energy at higher k values. This possible phenomenon is expected to be one of the reasons for the observed entropy values at $k > 0.15$.

4. Conclusions

A good design for the cell and understanding electrode polarizations are the key to obtaining meaningful thermodynamic data using coulometric titration cells. The interfacial contact between Li-β'' alumina electrolyte and IDβ'' alumina electrode is the main concern for the useful operational life of the cell. In the present work with coulometric titration cells, two new techniques, hot pressing and glass sealing, were developed to obtain a suitable and stable Li-β'' alumina/IDβ'' alumina interface. The variation of the equilibrium cell e.m.f. with sodium content and temperature was determined. Four discharge and three charge cycles were applied to demonstrate the reversibility of the cell. The width of homogeneous ranges of IDβ'' alumina with changes in sodium content were determined over the temperature range of 444–523 K. These homogeneous ranges were strongly dependent on ferrous iron content in IDβ'' alumina. The good storage capacity of the IDβ'' alumina was proved and it was indicated that IDβ'' alumina is a good solid solution material for electrochemical devices utilizing sodium β-alumina type electrolytes. Using the e.m.f. values obtained in the present investigation, the sodium activity in the IDβ'' alumina and the partial molar thermodynamic quantities, $\overline{\Delta G}_{Na}$, $\overline{\Delta H}_{Na}$ and $\overline{\Delta S}_{Na}$ were calculated as a function of composition and temperature.

The entire area of non-stoichiometric materials represents a significant challenge to thermodynamicists [17]. It is almost impossible to treat grossly non-stoichiometric compounds in terms of ideal solutions of point defects. A better understanding of defect structure and electronic properties of IDβ'' alumina are needed to explain the broad range of non-stoichiometric IDβ'' alumina and the non-linear thermodynamic quantities, $\overline{\Delta H}_{Na}$ and $\overline{\Delta S}_{Na}$.

References

1. J. P. ROLAND, T. Y. TSENG and R. W. VEST, *J. Amer. Ceram. Soc.* **62** (1979) 567.
2. D. J. FRAY and B. SAVORY, *J. Chem. Thermo.* **7** (1975) 485.
3. L. HSUEH and D. N. BENNION, *J. Electrochem. Soc.* **118** (1971) 1129.
4. N. K. GUPTA and R. P. TISCHER, *ibid.* **119** (1972) 1033.
5. A. S. NAGELBERG and W. L. WORRELL, *J. Solid State Chem.* **29** (1979) 345.
6. G. J. DUDLEY, B. C. H. STEELE and A. T. HOWE, *ibid.* **18** (1976) 141.
7. D. S. EDDY and E. RUSCIOLELLI, General Motors Corp., Research Report, ET-127 (1977).
8. R. G. PASTOR, PhD thesis, Purdue University (1982).
9. W. L. ROTH and R. J. ROMANCZAK, *J. Electrochem. Soc.* **116** (1969) 975.
10. T. Y. TSENG, PhD. Thesis, Purdue University (1982).
11. D. H. EVERETT and W. I. WHITTON, *Trans. Faraday Soc.* **48** (1952) 749.
12. D. H. EVERETT and F. W. SMITH, *ibid.* **50** (1954) 187.
13. D. H. EVERETT, *ibid.* **50** (1954) 1077.
14. J. H. KENNEDY and A. F. SAMMELLS, *J. Electrochem. Soc.* **121** (1974) 1.
15. M. S. WHITTINGHAM, *ibid.* **123** (1976) 315.
16. K. ENDO, S. YAMAUCHI, K. FUEKI and T. MUKAIBO, *Bull. Chem. Soc. Japan* **49** (1976) 1191.
17. R. A. SWALIN, "Thermodynamics of Solids", 2nd edn (John Wiley, New York, 1972) p. 351.

Received 2 June
and accepted 22 October 1987